Limitation of spiral microchannels for particle separation in heterogeneous mixtures: impact of particles' size and deformability

Limitation of spiral microchannels for particle separation in heterogeneous mixtures: impact of particles' size and deformability

Ewa Guzniczak[1], Timm Krüger[2], Helen Bridle[1]* & Melanie Jimenez[3]

[1] Heriot-Watt University, School of Engineering and Physical Science, Department of Biological Chemistry, Biophysics and Bioengineering Edinburgh Campus, Edinburgh, EH14 4AS, Scotland

[2] School of Engineering, Institute for Multiscale Thermofluids, University of Edinburgh, Edinburgh EH9 3FB, Scotland

[3] Biomedical Engineering Division, James Watt School of Engineering, University of Glasgow, G12 8LT

* Corresponding author: Helen Bridle h.l.bridle@hw.ac.uk

Keywords

Spiral microchannel, size- and deformability-based particle separation, particle focussing, mixed population

Author Contributions

EG and MJ designed the presented experimental work, EG performed the experiments and data analysis. TK contributed to discussions regarding data analysis and interpretation. EG, TK, HB and MJ wrote the manuscript, with TK editing. HB and MJ are joint last authors.

Abstract

Spiral microchannels have shown promising results for separation applications. Hydrodynamic particle-particle interactions are a known factor strongly influencing focussing behaviours in inertial devices, with recent work highlighting how the performance of bidisperse mixtures is altered when compared with pure components, in square channels. This phenomenon has not been previously investigated in detail for spiral channels. Here, we demonstrate that, in spiral channels, both the proportion and deformability of larger particles (13 μm diameter) impact upon the recovery (up to 47% decrease) of small rigid particles (4 μm). The effect, observed at low concentrations (volume fraction <0.0012), is attributed to the hydrodynamic capture of beads by larger cells. These changes in particles focussing behaviour directly impede the efficiency of the separation – diverting beads from locations expected from measurements with pure populations to co-collection with larger cells – and could hamper deployment of the technology for certain applications. Similar focussing behaviour alterations were noted when working with purification of stem cell end products.

Introduction

Separation and sorting of cells is an important bioprocess across medical, environmental and biotechnology applications, where existing technologies like centrifugation and filtration have several drawbacks [1-3]. Microfluidic approaches to cell sorting and separation can be divided into active, which exploit external forces e.g., electrical, acoustic, optical or magnetic fields, and passive, which utilise channel geometry and hydrodynamic forces [4].

Inertial focussing has proved a popular passive method, delivering high-throughput separation of various particles from heterogeneous samples based upon their size, shape and deformability [1, 2, 5, 6]. Several different geometries have been investigated with the majority of studies falling into the classification of straight, serpentine or spiral channels [5]. These channels typically have a square or rectangular cross section, though trapezoidal [7] or triangular [8] cross sections have been investigated, along with contraction-expansion arrays [9]. The use of pillars within devices has also been exploited to manipulate the flow field to achieve solution exchange and particle separations [10].

Particle focussing within a spiral microchannel is determined by the particle properties and its interplay with the fluid dynamics within the confined channel geometry [11, 12]. Spirals are often selected for separation applications due to their high throughput [25] with details of the forces involved given in recent reviews covering theory [12-14], applications [1] and modelling [15]. At present, there is no tool to precisely predict focussing behaviours and locations of particles, in arbitrary systems, that could inform optimal design and flow rate for separation. The impact of having mixed populations in spiral microchannels has also not been investigated in depth in the literature. In our previous work however, we observed significant changes of separation efficiency when the end products of a stem cell differentiation process (cord blood CD34+ cells to red blood cells (RBCs)) were studied in a spiral as pure or mixed population [26]. Other examples are also available in the literature. In Bhagat et al [29], using a spiral with two inlets to separate 1.9 μm and 7.32 μm particles, the normalised particle distributions at the channel outlets are different in the pure samples (Fig. 4a and Fig. 5a in [29]), compared to the mixed sample (Fig. 7c in [29]). In addition, when Son et al [30] utilised a spiral set-up to isolate non-motile sperm from RBCs, differences were observed between pure sperm distribution across the channel (Fig. 3 in [30]) and samples of sperm mixed with blood (Fig. 5 in at 0.2 mL/min [30]). The comparison of Fig. 4(2) with Fig. 6(3) in Son et al [30] also shows a change in sperm behaviour with the use of mixed samples, with the sperm distribution altering to closely mirror that of the RBCs, although the only data for which the comparison is available (0.1 mL/min) is not an optimised condition for the device. Fuchs et al. [31] used a spiral channel to isolate fungal cells from

white blood cells, with the recovery of fungal cells reduced when comparing performance in phosphate-buffered saline (PBS) with performance in blood samples (Fig. 3 in [31]), a factor attributed to the viscosity of blood samples. Hou et al. adopted a cascaded system to completely remove RBCs from circulating tumour cells (CTCs); their results indicate that there was little difference in the focussing behaviour of the larger CTCs between PBS and blood samples, whereas RBCs could be found in the CTC outlet due to undesirable cell-cell interactions [32]. Other work by Hou et al [33] looked at smaller particle mixtures, attempting to separate bacteria from blood with a double inlet spiral that was designed and tested with pure populations; in a mixed sample, bacterial recovery was reduced to 75%, attributed to the RBCs hindering the complete Dean migration of bacteria towards the outer channel wall. Finally, Tallapragada [2] noted that, using particle mixtures, the Reynolds number required for separation is significantly higher than predicted from pure sample data. The authors state a rigorous analysis of the effect is left for future work but propose a hypothesis for this effect based on the interaction between the wake of particles in one focussed stream with those in another.

In order to better understand particle interactions, Gao et al. [16] recently explored the effect of bidisperse suspensions on inertial focussing behaviour within straight square channels, reporting that the inertial focussing positions were modified in comparison with performance in monodisperse conditions. A conference paper by the same group revealed that smaller particles are more impacted than larger particles [17]. It was shown that, as the ratio between particle sizes increased, the focussing position of the smaller particles was altered, in particular, the main four equilibrium positions were occupied by larger particles, and smaller particles remained concentrated on an annulus close to the channel walls.

Particle interactions are known to impact on behaviour within inertial focussing systems. For example, the formation of trains with evenly distributed particles in inertial focussing devices has been reported previously [16, 18]. Lee *et al.* proposed that inter-particle spacing is a consequence of particle-induced convection [19]. Viscous disturbance flow generated by a particle under confinement acts on a neighbour particle, repelling it a certain distance. Once particles assemble into a train with defined inter-particle spacing, this state is preserved by the action of inertial lift force [20]. When particles are too concentrated, alterations in the ordering of trains have also been observed [21]. The focussing positions of particles are also altered in the presence of a large number of other particles; for example, a novel focussing mode was observed for cancer cells in whole blood, that was not present in PBS and diluted blood [22], and others have described the mixing effect of RBC interactions at high haematocrit, reducing the inertial migration of cancer cells [23]. In straight channels,

incorporating local microstructures, the interaction between particles was noted to decrease the sorting purity and efficiency as particle concentration increased [24]. Wu et al [23, 24] also highlighted that small particles are particularly prone to be influenced by interactions with larger particles.

In the present paper we discuss how focussing of particles in spiral channels is altered in a heterogeneous mixture as compared to pure populations when the concentration of particles is kept constant at a low volume fraction. We obtained data on the recovery rates and focussing positions of both pure and mixed populations for 1) the end products of a stem cell differentiation process and 2) beads mixed with larger and softer cells. For all the tested cases, we demonstrate that a heterogeneous mixture of particles, of different size and deformability, behave significantly differently than pure populations, leading to significantly impeded separation efficiency. Further investigation of this phenomenon might consequently yield a new understanding of the limitations of inertial microfluidic devices.

Results

Focussing behaviour of stem cells

In [26], a microfluidic spiral channel was used to sort differentiating stem cells (cord blood CD34+ cells) and most specifically the following three populations: enucleated cells (the end product), nucleated cells and nuclei (Figure 1-a). We demonstrated that enucleated and nucleated cells have similar sizes (ca. 8 µm in diameter) but differ in their deformability, while nuclei are significantly smaller (ca. 5 µm in diameter). Operating conditions were optimised to maximise the enrichment of enucleated cells based on size and deformability differences, leading to a flow rate of 1 mL/min when analysing data with pure (pre-sorted) populations. The purity of enucleated cells – which was the main criterion investigated in our previous work – was surprisingly significantly lower than predicted (down to ca. 70%) when a mixed population (enucleated/nucleated cells and nuclei) was injected in the spiral. Interestingly, nuclei that were observed to focus towards the inner wall in pure populations were also found with enucleated cells in the outlet closest to the outer wall in mixed population experiments.

In order to better understand this phenomenon, we compared in the present work the recovery of each cell population in a mixed sample. A sample containing circa 10^6 cells/mL with 20% enucleated cells, 50% nucleated cells and 30% nuclei by number (following cord

blood CD34+ cells differentiation according to the protocol published in [10]) was injected into the spiral at 1 mL/min, with recoveries determined using flow cytometry.

***Figure 1**. Device design and stem cell performance. **a**. Schematic of the spiral channel used for stem cell sorting with a 170 µm × 30 µm rectangular cross-section, 6 loops, one inlet and four outlets. Enucleated and nucleated cells as well as nuclei – differentiated from cord blood CD34+ cells – are injected at 1 mL/min. **b**. Recovery of cells is measured in each outlet using flow cytometry for mixed populations. Bars represent the mean value, and error bars denote the standard deviation of the mean. **c**. Results from mixed populations ("Experimental") are compared to predicted recoveries from pure population data ("Predicted"). The device design was also utilised in [26] but the presented data was not published there.*

As depicted in Figure 1-b more cells than anticipated (+18.9% for nucleated cells and +1.4% for nuclei) travelled with enucleated cells to the outlet closest to the outer wall (outlet A) in a mixed population. A shift towards the outer wall was also observed for nuclei and nucleated cells, with a substantial depletion (-16.1% for nucleated cells and -24.0% for nuclei) from the outlet closest to the inner wall (outlet D). These results seem to confirm that the presence of other cells has the potential to alter focussing behaviours even when working at relatively low cell concentrations (see Table 1).

In order to better understand the impact of cell mixtures on recovery and consequently yield a new understanding of a potential limit of use associated with inertial focussing devices for separation, the goal was then to reproduce these tests with different particles. Figure 1 demonstrates that the biggest changes in focussing behaviours were observed for nucleated cells and nuclei. Although nuclei were closer – in terms of focussing position in the spiral – to nucleated cells, it remains unclear if this proximity was the only factor impacting their behaviours or if enucleated cells also had an influence. Consequently, a system with only two populations – rigid 4 µm beads and Jurkat cells – was used. Jurkat cells are 13 µm in diameter, which is larger than the 8 µm of cells previously used, and present a similar deformability to nucleated cells (Young's Modulus 0.87±0.03 kPa) [27]. Based on their size (compared to a channel height of 30 µm) and deformability, it was expected that Jurkat cells will tend to focus in the middle of the channel, similarly to what was observed (on average) for enucleated cells [10]. 4 µm spherical beads were expected to focus closer to the inner wall, similarly to nuclei. Since deformability also has a significant role in cell focussing [28],

experiments with fixed Jurkat cells (Young's Modulus 2.15±0.10 kPa) were performed for comparison.

It can be noted that the spiral was not redesigned to optimise the separation of Jurkat cells and beads; the proposed set-up aims to investigate whether changes observed with a heterogeneous stem cell sample are translatable to a different mixture of particles. Consequently, the same spiral (Figure 1-a) and total particle concentration (10^6 cells/mL) were used. More details on particle concentration, volume and line fractions for all the tested samples are presented in Table 1. Experiments with stem cells were done at 1 mL/min, which corresponds to a Reynolds number of 168 (the Reynolds number is defined as $Re = \rho U_{Max} D_h / \mu$, where ρ is the fluid density, μ is the fluid viscosity, U_{Max} is the maximum velocity of the fluid and D_h the hydraulic diameter of the channel). For beads and Jurkat cells, no significant changes in focussing were observed for Re above 66 (Figure S1).

Inlet sample	Composition of inlet sample	Volume fraction of inlet sample	Line fraction of inlet sample
Figure 1			
Enucleated cells	100%	0.000268	0.020
Nucleated cells	100%	0.000268	0.020
Nuclei	100%	0.000065	0.008
Enucleated cells + Nucleated cells + Nuclei	20% 50% 30%	0.000053 0.000134 0.000019	0.004 0.008 0.003
Figure 2			
4 µm beads	100%	0.000034	0.010
Jurkat cells	100%	0.001150	0.033
Figure 3			
Beads + Jurkat cells	60% 40%	0.000020 0.000460	0.006 0.013
Beads + Jurkat cells	40% 60%	0.000013 0.000690	0.004 0.020
Beads + Jurkat cells	20% 80%	0.000007 0.000920	0.002 0.026
Figure 4			
Beads + stiff Jurkat cells	75% 25%	0.000025 0.000288	0.006 0.007

Beads + stiff Jurkat cells	50% 50%	0.000017 0.000575	0.004 0.013
Beads + stiff Jurkat cells	25% 75%	0.000008 0.000863	0.002 0.020

Table 1*. Characteristics of the samples tested in this work. All samples contain either a pure or mixed population of particles diluted in PBS to a total concentration of 10^6 particles/mL. For mixed populations, composition % reports the particle number of each subpopulation divided by the total number of particles in the sample. For line fractions, 2 focussing positions are assumed.*

Focussing behaviour of pure populations of Jurkat cells and 4 µm spherical polystyrene beads

The focussing behaviour of single populations of beads and Jurkat cells at Re=66 is presented in Figure 2-a. By quantifying the number of cells imaged in four equal sections within the channel cross-section (corresponding to the four outlets of the device), it could be predicted that 100% of beads would be collected in outlet D, the closest outlet to the inner wall, while soft and stiff cells should be mainly distributed between outlets B and C, the middle outlets (predicted recovery of Jurkat cells in outlet B: 68% and outlet C: 28%; predicted recovery for stiff Jurkat cells in outlet B: 36% and outlet C: 48%). As shown in Figure 2-b, experiments collecting and quantifying outlet samples confirmed that – for pure populations – 100% of the beads are indeed collected in outlet D. Cells remain closer to the centreline and are mostly collected in outlets B and C. 63±3% of Jurkat cells travel to outlet B and 27±3% to outlet C. As previously observed [11], changes in deformability can alter focussing behaviours, and a larger number of stiffer Jurkat cells are collected in outlet C (48±6%). Only a small portion of both cell types are directed to the outermost outlets A and D. These experimental results, from collected outlets, are in line with the predicted recovery, from imaging, of beads/cells with a minimal error (0.5±0.7%). By gaining information on the focussing behaviours of pure populations, it will be possible next to evaluate whether 1) mixing beads and cells do alter particle recovery and 2) proximity in focussing positions has an impact (stiffer Jurkat cells having a closer distance to beads than control (soft) Jurkat cells have to beads).

Figure 2*. Pure population behaviours.* ***a****. Position of pure populations of 4 µm beads (green), soft (orange) and stiff (blue) Jurkat cells assessed at Re=66 using high speed imaging. The lateral equilibrium position was measured as a distance from the outer wall (µm) at the end of the spiral channel and was generated by image analysis.* ***b****. The recovery in each outlet of the spiral is measured by analysing the sample post-processing. Bars*

represent the mean value, and error bars denote the standard deviation of the mean. Red horizontal bars represent the predicted recovery from focussing positions inside the channel.

Focussing behaviour of mixed populations of control (soft) Jurkat cells and 4 µm spherical polystyrene beads

Mixtures were prepared with 4 µm beads and Jurkat cells at varying cell/bead number ratios (*cf*. Table 1). The hydrodynamic behaviour of particles in a mixed population is depicted in Figure 3-a.

For all the tested conditions, the distribution of 4 µm beads within the channel cross-section was altered by the presence of Jurkat cells. When run as a pure sample, beads were focused in a tight stream close to the inner wall of the channel (75% of all events being focused at 158–160 µm). In the presence of Jurkat cells, beads occupy a wider section of the channel with 75% of beads occupying a lateral position distributed between 80–161 µm. In comparison, the larger Jurkat cells remain mostly focused at the centre of the channel for pure and mixed samples.

As presented in Figure 3-b, the recovery of beads in outlet D dropped from 100% (pure population) to <70% in the presence of Jurkat cells for all the tested concentrations. Moderate changes are also observed for the recovery of cells, with a small increase (0.3-1.3%) of cells collected in outlet D for all the tested conditions. The most noticeable change was recorded in outlet B, with up to 15% depletion of cells in favour of flanking outlets C and A when cells outnumbered beads.

Figure 3*. Mixed population behaviour with soft cells* ***a****. Position of 4 µm beads (green), soft Jurkat cells (orange) in the spiral at Re=66 for bead/cell ratios of 60%/40% (left panel), 40%/60% (mid panel) and 20%/80% (right panel).* ***b****. The corresponding recovery in each outlet of the spiral is measured and compared to data from pure population (red horizontal lines represent the predicted recovery from focussing positions inside the channel for pure populations). Bars represent the mean value, and error bars denote the standard deviation of the mean.*

Focussing behaviour of mixed populations of stiff Jurkat cells and 4 µm spherical polystyrene beads

Similar conclusions can be drawn for mixtures with stiffer Jurkat cells (Figure 4). Fewer beads are recovered in outlet D in the presence of cells, although interestingly the loss is less significant than with soft Jurkat cells (where the lowest recovery of beads is 53±4% with soft cells compared to 62±1% with stiff cells). For stiff Jurkat cells it would appear that increasing cell concentration leads to slightly lower bead recovery rates in outlet D. More stiff cells are also collected in outlet D for the highest cell/bead ratios. Similarly to soft cells, stiff cells were slightly depleted from outlets B and C in favour of the outlets A and D.

Figure 4*. Mixed population behaviour with stiff cells* ***a****. Position of 4 µm beads (green), stiff Jurkat cells (blue) in the spiral at Re=66 for bead/cell ratios of 75%/25% (left panel), 50%/50% (mid panel) and 25%/75% (right panel).* ***b****. The corresponding recovery in each outlet of the spiral is measured and compared to data from pure population (red horizontal lines represent the predicted recovery from focussing positions inside the channel for pure populations). Bars represent the mean value and error bars, the standard deviation of the mean.*

Discussion

In microfluidics, particles constitute an active component of the system shaping and altering the fluid flow pattern [11]. From the results reported above, it can be concluded that with pure populations – and in the tested spiral design – small particles (beads or nuclei) focus tightly against the inner wall, while larger cells remain closer to the centreline or outer wall, depending on their size/deformability. In mixed populations, we observed significant alteration in focussing behaviours for 13, 8 and 5 µm biological cells as well as 4 µm rigid beads. For tests with beads and Jurkat cells, we observed that this impact, especially on bead loss in the predicted outlet, reduced recoveries to <70% in all cases. Comparing the influence of deformability on this behaviour, it would seem that softer cells have a greater impact. To the best of our knowledge, the interaction between heterogeneous mixtures within spiral channels has not been previously discussed in the literature. However, there is evidence, as highlighted in the Introduction, where the performance of mixed populations is reduced compared to that of pure populations [29-32]. In several of these examples it appears to be the smaller particle behaviour which is most altered, e.g. sperm cells distribution reflecting that of RBCs [30] and RBCs being found in the CTC collection channel [32]. In this latter example the behaviour was attributed to undesirable cell-cell interactions. Additionally, Tallapragada et al [2] identify that higher Reynolds numbers are needed for

effective separation in mixed samples compared with pure counterparts, and conclude this is due to interactions between the wakes of particles.

According to images recorded inside the channel (Figure 5), cells in the spiral tested here seem to form trains and capture some of the smaller particles. Capture here does not imply physical contact; it is rather associated with the phenomenon of a small particle being "hijacked" by a larger particle, deviating the small particle from the equilibrium position it would have in a pure population. The formation of trains with evenly distributed particles in inertial focussing devices has been reported previously [16]. Lee *et al.* [19] proposed that inter-particle spacing is a consequence of particle-induced convection. Viscous disturbance flow generated by a particle under confinement acts on a neighbour particle, repelling it a certain distance. Once particles assemble into the train with defined inter-particle spacing, this state is preserved by the action of inertial lift force [20]. Changes in the ordering of trains have also been observed when particle concentrations become too high [21]. In straight channels it has previously been observed that high concentrations of particles can lead to alterations in focussing behaviour and positions [23,24].

In this work, however, the concentration was kept low, 10^6 cells/mL, with corresponding volume and line fractions detailed in Table 1. As the cell/bead ratio increases, it can be seen that the total volume fraction increases, which could potentially play a role in the observed effects. However, the total volume fractions remain relatively low in comparison to previous work where the impact of particle concentration on inertial focussing performance has been observed. Inter-particle distances of less than 10 particle diameters could affect the equilibrium position and axial spacing between other particles, with many of the articles reporting trains doing so inter-particle distances of about 5 particles (line fraction of 1/6) [18]. However as can be seen in Table 1 the largest line fraction in this work is around 1/30, illustrating that the observed effects cannot be explained by crowding within a given line.

This mechanism of hydrodynamic interactions influencing focussing positions appears different to the recent work of Gao et al. [16] investigating bidisperse mixtures in square straight channels, where the larger particles occupy the four main focussing positions and the smaller particles thus remain on an annulus close to the channel wall.

Figure 5. *Examples of images of 4* μm *beads and larger Jurkat cells at Re=66 where the deviation of beads from the inner wall (right-hand side of the images) is visible. The left*

image is from the case of control (soft) Jurkat cells and the right image is with stiffer Jurkat cells, both from the situation where there are a greater number of beads than cells though similar images can be found for all cell/bead ratios.

Although it was not possible to confirm by imaging the capture of nucleated cells by enucleated cells (these cells having the same size, it can be challenging to distinguish them using bright-field imaging only), results from Figure 1 seem to confirm that alteration of focussing positions is not limited to small particles. The size ratio between particles should, however, play a significant role in the capture, explaining the appearance of small beads within the trains of the large cells while the spatial distribution of the cells is only moderately affected by the presence of the beads; we did not identify cells joining trains of 4 μm beads focused near the inner wall of the channel. A profound understanding of these effects would aid better control inertial device performance.

Conclusion

We presented evidence of alterations in focussing behaviour and separation efficiency in a spiral inertial focussing channel at low volume fractions when the performance of a heterogeneous particle mixture is compared to the individual particle populations. Both the size and deformability of particles within the mixture have an influence. In a scenario where small beads are mixed with larger cells, hydrodynamic particle-particle interactions, in which smaller particles can be self-assembled into trains of the larger particles, adversely affect particle separation in the spiral microchannel. Effects have also been observed for larger cells presenting different deformability (and hence focussing at different positions in the channel). The mixing effect could be desirable for certain applications; however, these poorly understood factors altering focussing positions of particles in inertial sorters can constitute a significant fundamental issue. Improved understanding of these effects would aid better control over inertial devices performance and facilitate making inertial focussing a mainstream technology in the future.

Materials and methods

Cell preparation

Enucleated, nucleated cells and nuclei for Figure 1 were prepared according to the protocol published in [26]. Jurkat cells were washed twice in PBS-/- (phosphate buffered saline without calcium and magnesium, Gibco), re-suspended at 1×10^6 cell/mL in PBS-/-. For work

with stiff Jurkat cells, cells were supplemented with 0.1% (v/v) Glutaraldehyde (SigmaAldrich), incubated at room temperature for 40 min, washed once in PBS-/- and re-suspended in PBS-/- supplemented with 0.1% Pluronic F-68 (ThermoFisher Scientific). The deformability of Jurkat cells with and without treatment was measured using real-time deformability cytometry, with Young modulus estimated using a build-in algorithm [28, 34].

Bead preparation

4µm beads (Magsphere Ltd.) were either diluted in PBS or diluted with cells; the total particle concentration was kept to 1×10^6 cell/mL.

Hydrodynamic behaviour in spiral microchannel

Samples were injected into the microfluidic device with a mid-pressure syringe pump (neMESYS 1000N, Cetoni, Germany) through 1/16" PTFE tubing (Thames Restek, UK). The hydrodynamic behaviour of particles was assessed in terms of lateral equilibrium position (measured as a distance from the particle centre to the channel outer wall [µm]) measured at the end of the spiral channel by high-speed microscopic imaging. Images were recorded at ×20 magnification using an objective with a 4.9 mm free working distance (421251-9911-000 LD A-Plan 20x Ph1, Zeiss) by a high-speed CMOS camera (MC1362, Mikrotron, Germany) mounted on a microscope (Zeiss Axio Observer 3, Zeiss, Germany) at 2000 frames per second. Lateral positions within the channel were recorded for more than 10,000 events at three independent occasions, for each researched condition, using a custom-written program ShapeIn and quantified using the software ShapeOut version 0.8.4 (available at www.zellmechanik.com).

Separation efficiency

Separation efficiencies after processing in the spiral channel were quantified by flow cytometry. The recovery in each outlet for a particle type [P] is defined as

$$Recovery[P]_{outlet_i} = \frac{[P]_{outlet_i}}{\sum_{i=1}^{4}[P]_{outlet_i}} \quad (1)$$

Data analysis and plotting were performed using GraphPad Prism 6 and FlowJo V10 CL.

Supplementary Material

See supplementary material for the hydrodynamic behaviour of pure populations at different flow rates.

Acknowledgements

EG and HB would like to thank IBioIC and Epigem for the PhD studentship. TK received funding from the European Research Council (ERC) under the European Union's Horizon 2020 research and innovation programme (Grant agreement No. 803553). MJ was supported by the Royal Academy of Engineering under the Research Fellowship scheme ((RF/201718/1741). MJ would also like to thank the Engineering and Physical Sciences Research Council (EPSRC) and the Royal Society for their support (EP/R006482/1 and RGS\R1\191188).

Data Availability

The data that support the findings of this study are available from the corresponding author upon reasonable request.

Bibliography

1. Herrmann, N., P. Neubauer, and M. Birkholz, *Spiral microfluidic devices for cell separation and sorting in bioprocesses.* Biomicrofluidics, 2019. **13**(6): p. 061501.

2. Tallapragada, P., et al., *Scale invariant hydrodynamic focussing and sorting of inertial particles by size in spiral micro channels.* Journal of Micromechanics and Microengineering, 2015. **25**(8): p. 084013.
3. Zhang, J., et al., *Inertial particle separation by differential equilibrium positions in a symmetrical serpentine micro-channel.* Scientific Reports, 2014. **4**(1): p. 4527.
4. Wyatt Shields Iv, C., C.D. Reyes, and G.P. López, *Microfluidic cell sorting: a review of the advances in the separation of cells from debulking to rare cell isolation.* Lab on a Chip, 2015. **15**(5): p. 1230-1249.
5. Gou, Y., et al., *Progress of Inertial Microfluidics in Principle and Application.* Sensors (Basel, Switzerland), 2018. **18**(6): p. 1762.
6. Zhang, J., et al., *High-Throughput Separation of White Blood Cells From Whole Blood Using Inertial Microfluidics.* IEEE Transactions on Biomedical Circuits and Systems, 2017. **11**(6): p. 1422-1430.
7. Warkiani, M.E., et al., *Slanted spiral microfluidics for the ultra-fast, label-free isolation of circulating tumor cells.* Lab on a Chip, 2014. **14**(1): p. 128-137.
8. Mukherjee, P., et al., *Single stream inertial focussing in low aspect-ratio triangular microchannels.* Lab on a Chip, 2019. **19**(1): p. 147-157.
9. Wang, X., J. Zhou, and I. Papautsky, *Vortex-aided inertial microfluidic device for continuous particle separation with high size-selectivity, efficiency, and purity.* Biomicrofluidics, 2013. **7**(4): p. 44119-44119.
10. Amini, H., et al., *Engineering fluid flow using sequenced microstructures.* Nature Communications, 2013. **4**(1): p. 1826.
11. Di Carlo, D., et al., *Continuous inertial focussing, ordering, and separation of particles in microchannels.* Proceedings of the National Academy of Sciences, 2007. **104**(48): p. 18892.
12. Gossett, D.R. and D.D. Carlo, *Particle Focussing Mechanisms in Curving Confined Flows.* Analytical Chemistry, 2009. **81**(20): p. 8459-8465.
13. Stoecklein, D. and D. Di Carlo, *Nonlinear Microfluidics.* Analytical Chemistry, 2019. **91**(1): p. 296-314.
14. Chung, A.J., *A Minireview on Inertial Microfluidics Fundamentals: Inertial Particle Focussing and Secondary Flow.* BioChip Journal, 2019. **13**(1): p. 53-63.
15. Razavi Bazaz, S., et al., *Computational inertial microfluidics: a review.* Lab on a Chip, 2020. **20**(6): p. 1023-1048.
16. Gao, Y., et al., *Inertial lateral migration and self-assembly of particles in bidisperse suspensions in microchannel flows.* Microfluidics and Nanofluidics, 2019. **23**(7): p. 93.
17. Tohme Tohme, et al., *Inertial migration of bidisperse suspensions flowing in microchannels: effect of particle diameters ratio*, in *European Conference on Fluid-Particle Separation*. 2018: Lyon.
18. Amini, H., W. Lee, and D. Di Carlo, *Inertial microfluidic physics.* Lab on a Chip, 2014. **14**(15): p. 2739-2761.
19. Lee, W., et al., *Dynamic self-assembly and control of microfluidic particle crystals.* Proceedings of the National Academy of Sciences, 2010. **107**(52): p. 22413.
20. Schaaf, C., F. Rühle, and H. Stark, *A flowing pair of particles in inertial microfluidics.* Soft Matter, 2019. **15**(9): p. 1988-1998.
21. Humphry, K.J., et al., *Axial and lateral particle ordering in finite Reynolds number channel flows.* Physics of Fluids, 2010. **22**(8): p. 081703.
22. Lim, E.J., et al., *Visualization of microscale particle focussing in diluted and whole blood using particle trajectory analysis.* Lab on a Chip, 2012. **12**(12): p. 2199-2210.
23. Tanaka, T., et al., *Inertial migration of cancer cells in blood flow in microchannels.* Biomedical Microdevices, 2012. **14**(1): p. 25-33.
24. Wu, Z., et al., *Continuous inertial microparticle and blood cell separation in straight channels with local microstructures.* Lab on a Chip, 2016. **16**(3): p. 532-542.

25. Liu, N., et al., *Spiral Inertial Microfluidics for Cell Separation and Biomedical Applications*, in *Applications of Microfluidic Systems in Biology and Medicine*, M. Tokeshi, Editor. 2019, Springer Singapore: Singapore. p. 99-150.
26. Guzniczak, E., et al., *Purifying stem cell-derived red blood cells: a high-throughput label-free downstream processing strategy based on microfluidic spiral inertial separation and membrane filtration.* Biotechnology and Bioengineering, 2020. **n/a**(n/a).
27. Guzniczak, E., et al., *High-throughput assessment of mechanical properties of stem cell derived red blood cells, toward cellular downstream processing.* Scientific Reports, 2017. **7**(1): p. 14457.
28. Guzniczak, E., et al., *Deformability-induced lift force in spiral microchannels for cell separation.* Lab on a Chip, 2020. **20**(3): p. 614-625.
29. Bhagat, A.A.S., S.S. Kuntaegowdanahalli, and I. Papautsky, *Continuous particle separation in spiral microchannels using dean flows and differential migration.* Lab on a Chip, 2008. **8**(11): p. 1906-1914.
30. Son, J., et al., *Non-motile sperm cell separation using a spiral channel.* Analytical Methods, 2015. **7**(19): p. 8041-8047.
31. Fuchs, B.B., et al., *Rapid Isolation and Concentration of Pathogenic Fungi Using Inertial Focussing on a Chip-Based Platform.* Frontiers in Cellular and Infection Microbiology, 2019. **9**(27).
32. Hou, H.W., et al., *Isolation and retrieval of circulating tumor cells using centrifugal forces.* Scientific Reports, 2013. **3**(1): p. 1259.
33. Hou et al, Direct detection and drug-resistance profiling of bacteremias using inertial microfluidics, Lab Chip, 15, 2297-2307 (2015)
34. Mietke, A., et al., *Extracting Cell Stiffness from Real-Time Deformability Cytometry: Theory and Experiment.* Biophysical journal, 2015. **109**(10): p. 2023-2036.

a.

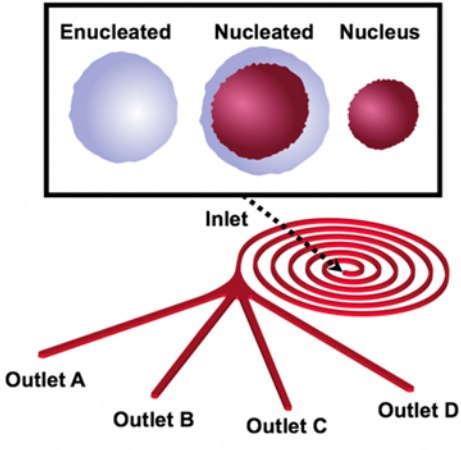

b.

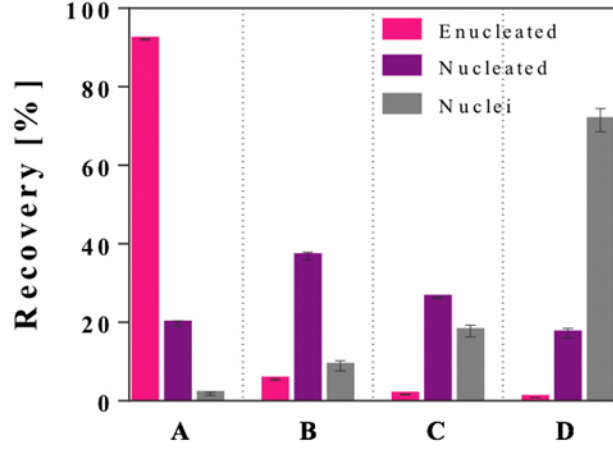

c.

Recovery [%]	Enucleated				Nucleated				Nuclei			
Outlet	A	B	C	D	A	B	C	D	A	B	C	D
Predicted	82.9	13.4	1.9	1.9	0.8	35.7	30.2	33.3	0.4	2.5	1.6	95.5
Experimental	92.1	5.5	1.6	0.8	19.7	36.8	26.3	17.2	1.8	8.9	17.8	71.5
Difference	9.2	-7.9	-0.3	-1.1	18.9	1.1	-3.9	-16.1	1.4	6.4	16.2	-24

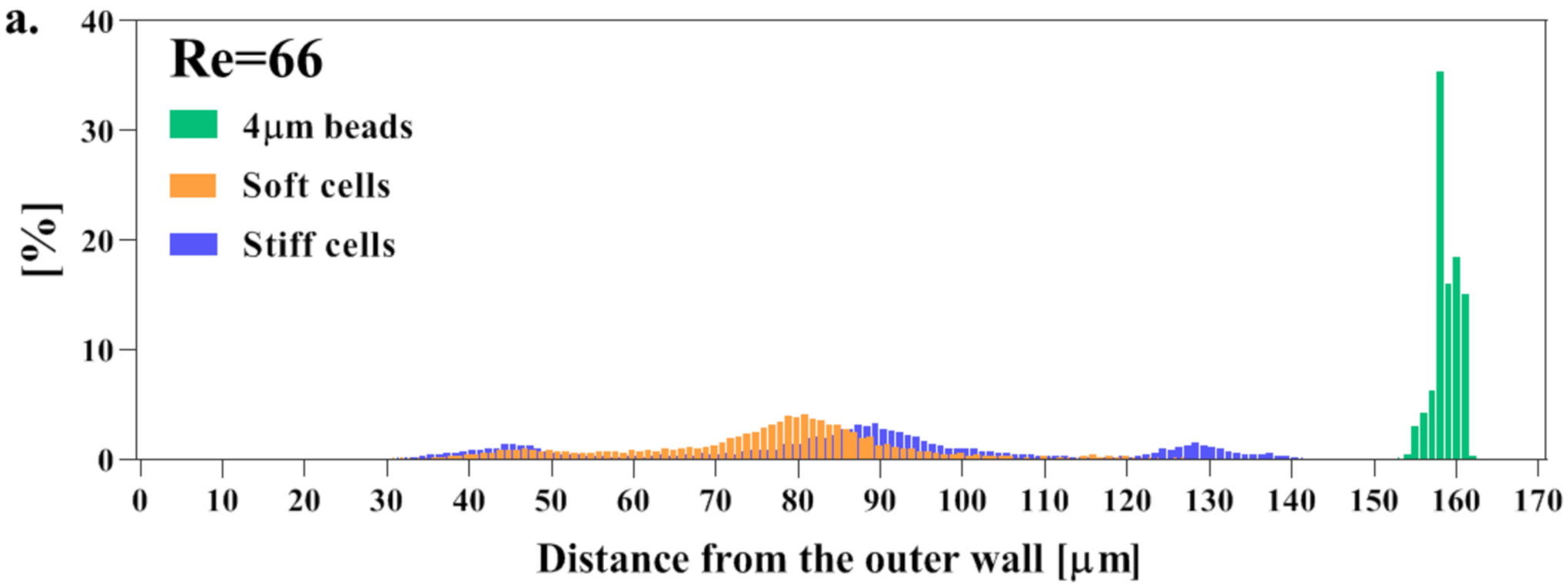

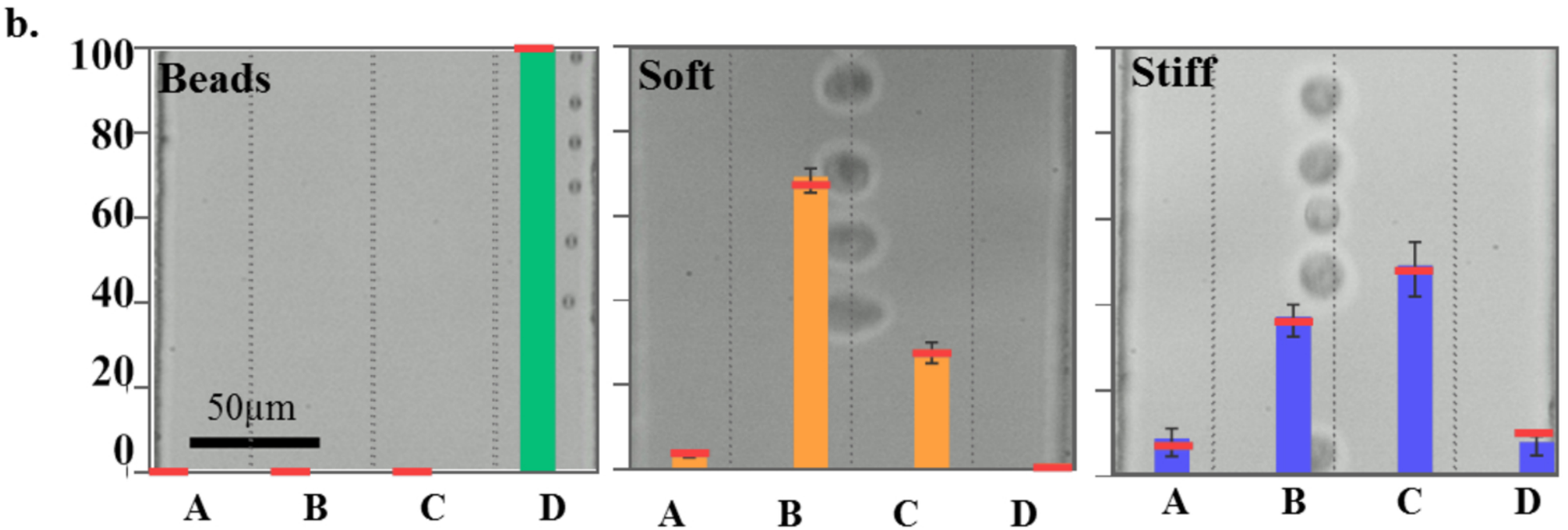

Predicted recovery obtained from pure samples

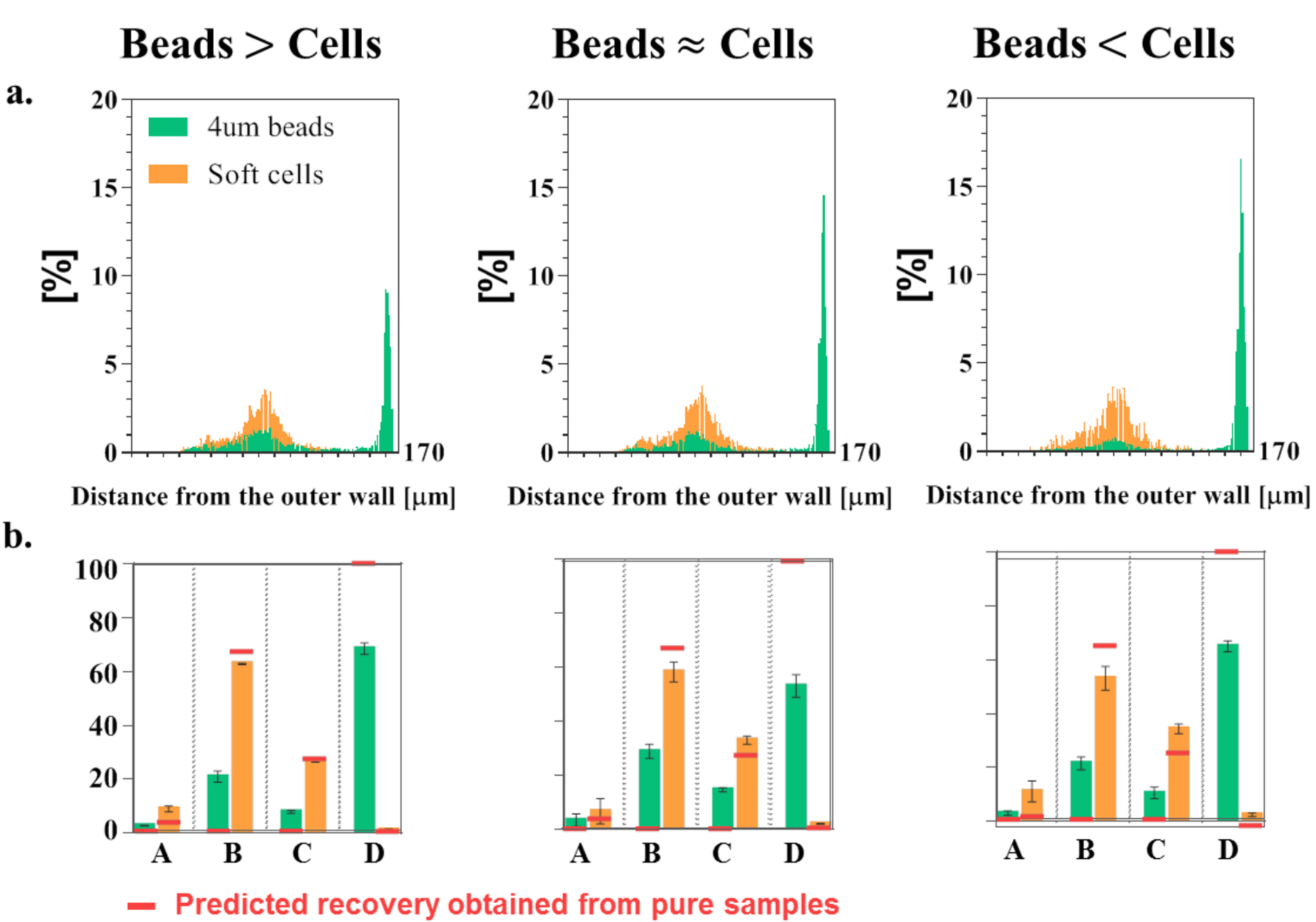
Beads > Cells
Beads ≈ Cells
Beads < Cells
a.
4um beads
Soft cells
[%]
20
15
10
5
0
170
Distance from the outer wall [µm]
b.
100
80
60
40
20
0
A
B
C
D
Predicted recovery obtained from pure samples

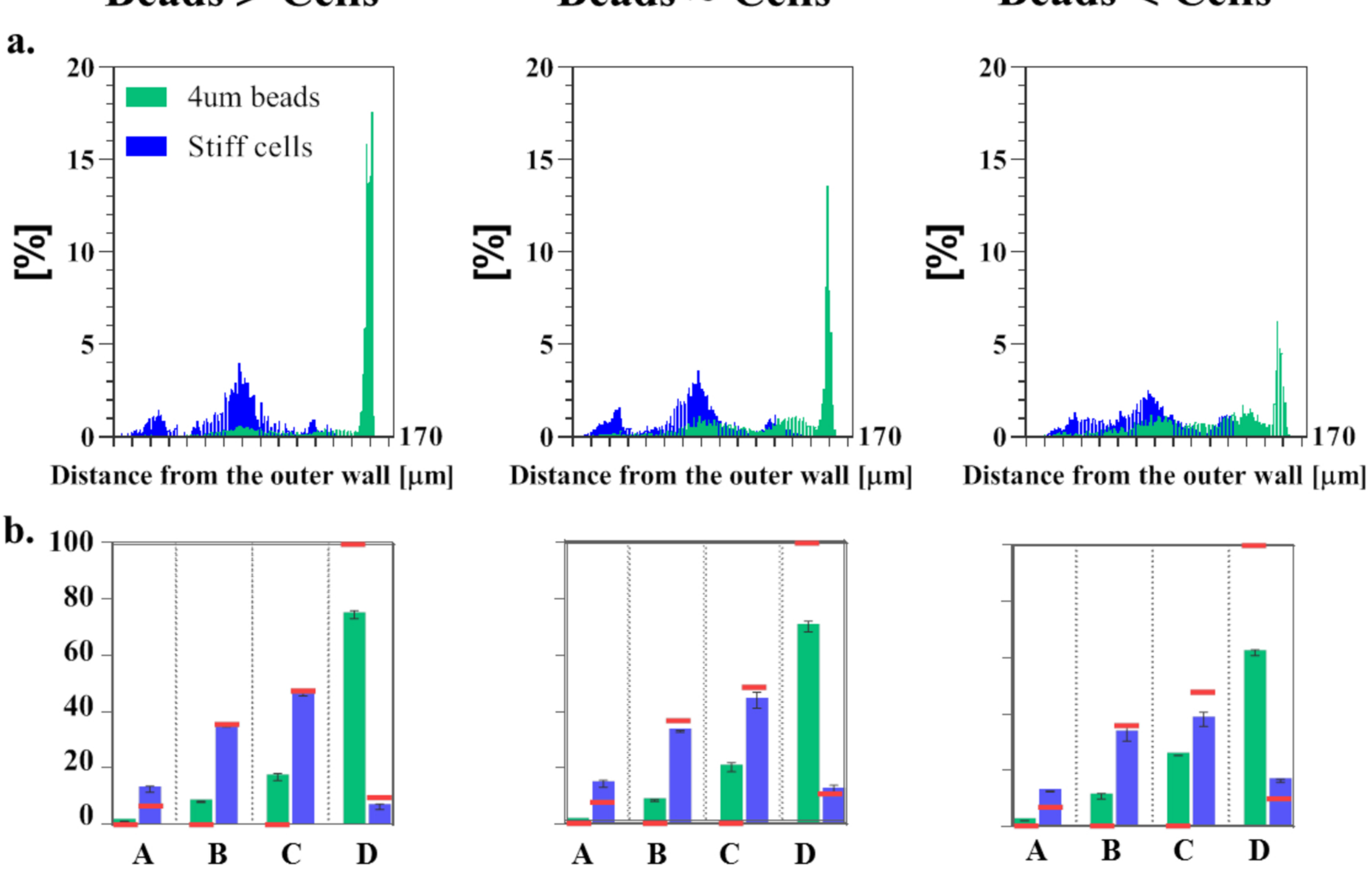
Beads > Cells
Beads ≈ Cells
Beads < Cells
a.
4um beads
Stiff cells
[%]
20
15
10
5
0
170
Distance from the outer wall [μm]
b.
100
80
60
40
20
0
A
B
C
D
Predicted recovery obtained from pure samples

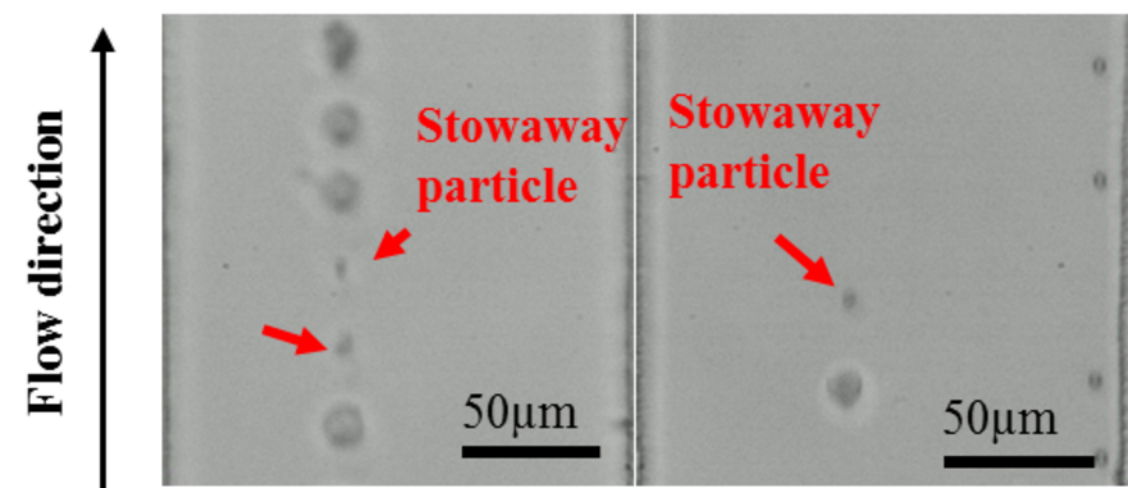
Flow direction
Stowaway particle
50μm
Stowaway particle
50μm